ITU Journal of Metallurgy and Materials Engineering

ITU/MMEJ

Effect of He^{+2}, Electron and Proton Particles on Polyvinyl Chloride

Zübeyde ÖZKAN[1]

[1]Gazi University, Graduate School of Natural and Applied Sciences, 06500 Ankara, Türkiye.

Abstract: Polyvinyl chloride (PVC) is widely used in many sectors (construction and building sector (pipe, sealing elements, etc.), electrical and electronics (cable, insulation material etc.), healthcare sector (serum bag, blood bag, etc.), automotive (wicks, coatings, etc.), furniture and decoration, consumer goods (hose, plastic tablecloth, some toys etc.) etc.) and has become an indispensable part of our daily lives. The interaction of polyvinyl chloride with photon-derived radiation, such as gamma rays and X-rays, has been extensively studied in the literature. Therefore, PVC was analysed using the NIST database-based PSTAR (proton)/ ESTAR (electron) / ASTAR (He^{+2}) programs for total stopping power (TSP), range, detour factor, density effect parameter, and radiation yield parameters against electrons, protons, and alpha (He^{+2}) particles in the energy range of 0.001 Mega-electron Volt (MeV) to 10000 MeV. Additionally, the SUSPRE (Surrey University Sputter Profile From Energy Deposition) simulation program was used to investigate the energy deposited in the material by He^{+2} at 100 MeV and its concentration values, which vary with depth. Polyvinyl chloride material has CSDA range values in the range of 2.974×10^{-4} g/cm^2 - 8.247×10^{1} g/cm^2 in response to the changing kinetic energies of electrons. The CSDA range values of proton particles vary between 7.734×10^{-6} g/cm^2 and 5.246×10^{3} g/cm^2. While the polyvinyl chloride material had the highest total stopping power value in He^{+2}, it had the highest range value in electrons. The radiation yield of the polyvinyl chloride material increased with the increase in the kinetic energy of the electron.

Keywords: PVC, SUSPRE, ESTAR, PSTAR, ASTAR.

He^{+2}, Elektron ve Proton Parçacıklarının Polivinil Klorür Üzerindeki Etkisi

Özet: Polivinil klorür (PVC), birçok sektörde (inşaat ve yapı sektörü (boru, sızdırmazlık elemanları vb.), elektrik ve elektronik (kablo, izolasyon malzemesi vb.), sağlık sektörü (serum torbası, kan torbası vb.), otomotiv (fitiller, kaplamalar vb.), mobilya ve dekorasyon, tüketim malları (hortum, plastik masa örtüsü, bazı oyuncaklar vb.) yaygın olarak kullanılmakla birlikte günlük hayatımızın vazgeçilmez bir parçası haline gelmiştir. Polivinil klorürün gama ışınları ve X ışınları gibi foton kaynaklı radyasyonla etkileşimi literatürde kapsamlı bir şekilde incelenmiştir. Bu sebeple, PVC, 0,001 Megaelektron Volt (MeV) ile 10000 MeV enerji aralığında elektronlara, protonlara ve alfa (He^{+2}) parçacıklarına karşı toplam durdurma gücü (TSP), menzil, sapma faktörü, yoğunluk etkisi parametresi ve radyasyon verimi parametreleri için NIST veri tabanına dayalı PSTAR (proton)/ ESTAR (elektron) / ASTAR (He^{+2}) programları kullanılarak analiz edildi. Ek olarak, 100 MeV'de, He^{+2} tarafından malzemeye bırakılan enerjiyi ve derinlikle değişen konsantrasyon değerlerini araştırmak için SUSPRE (Surrey Üniversitesi Enerji Biriktirmesinden Elde Edilen Püskürtme Profili) simülasyon programı kullanıldı. Polivinil klorür malzemesi, elektronların değişen kinetik enerjilerine yanıt olarak $2,974\times10^{-4}$ g/cm^2 - $8,247\times10^{1}$ g/cm^2 aralığında CSDA menzil değerlerine sahiptir. Proton parçacıklarının CSDA menzil değerleri $7,734\times10^{-6}$ g/cm^2 ile $5,246\times10^{3}$ g/cm^2 arasında değişmektedir. Polivinil klorür malzemesi He^{+2}'de en yüksek toplam durdurma gücü değerine sahipken, elektronlarda ise en yüksek menzil değerine sahiptir. Polivinil klorür malzemesinin radyasyon verim, elektronun kinetik enerjisindeki artışla birlikte artmıştır.

Anahtar Kelimeler: PVC, SUSPRE, ESTAR, PSTAR, ASTAR.

Research Article

Corresponding Author: Zübeyde Özkan, E-mail: zubeydeozkan@gazi.edu.tr

Reference: Özkan, Z., (2026). Effect of He^{+2}, Electron and Proton Particles on Polyvinyl Chloride, *ITU Journal of Metallurgy and Materials Engineering*, 3(2), 38-46.DOI: 10.65774/itummej.1956949.

Submission Date: 22 May 2026
Online Acceptance: 7 July 2026
Online Publishing: 29 July 2026

1.Introduction

Radiation is used in many applications, including the diagnosis and treatment of diseases, agriculture, food technology, archaeology (for artifact dating), industry, nuclear power generation, and seawater desalination [1–5]. Despite its numerous benefits, radiation may also have harmful effects. Depending on factors such as exposure duration, absorbed dose, and radiation type, radiation can adversely affect both humans and electronic devices [1,6]. Lead and lead-based materials have traditionally been used for radiation shielding because of their excellent attenuation properties. However, lead is toxic and poses environmental and health concerns. Therefore, scientists have made remarkable efforts to develop alternative materials with effective radiation shielding capabilities. These materials include glasses, alloys, thin films, and polymers [1–6].

Polymers are among the promising materials investigated for radiation shielding applications. Nylon-6, polyvinyl alcohol, and polyethylene are examples of polymers studied for this purpose. PVC, a polymer derived from a chlorinated hydrocarbon, was first commercially produced in 1930. It is widely used because of its favourable properties, including low weight, flexibility, low production cost, good mechanical performance, high flame retardancy, and excellent corrosion resistance. PVC is insoluble in water and most acids and organic solvents but exhibits limited solubility in tetrahydrofuran (THF) at room temperature. PVC materials are widely used in construction, medical devices, door and window frames, chemical processing equipment, food packaging, electrical insulation, piping systems, roofing materials, and many other applications [7–14].

Due to their low atomic numbers (Z), polymers alone cannot provide sufficient shielding against electromagnetic radiation such as gamma rays and X-rays. However, their radiation shielding performance can be significantly improved by incorporating high-Z fillers into composite materials, which enhance photon interactions through mechanisms such as the photoelectric effect, Compton scattering, and pair production. In neutron shielding applications, polymer materials effectively slow incoming neutrons because of the presence of light elements, such as hydrogen and carbon, in their structures [15–18]. The interaction mechanisms of polymeric materials with different types of radiation, including protons, alpha particles, and electrons, are examined in detail in this study.

Darki et al. [19] investigated the gamma-shielding properties of PVC composites reinforced with PbO and WO_3 and reported that increasing the filler content enhanced the shielding performance of the composites. Hadjal et al. [20] examined the effects of HfC, WC, and TaC fillers on the gamma-shielding properties of PVC-based composites and found that these additives improved gamma-ray attenuation by increasing photon–matter interactions. Mansy et al. [21] investigated the interactions of protons and alpha particles with matter and their mass stopping powers (MSP) in shielding materials. They reported that these interactions are primarily governed by Coulomb forces between positively charged particles and atomic electrons. Tahir et al. [22] studied the electron stopping powers of PMMA, PE, and PVC in the energy range of 200 eV–50 keV and observed that stopping power decreased with increasing electron energy. Perişanoğlu [23] reported that the MSP values of metallic glasses increased with particle kinetic energy up to a certain level and subsequently decreased. He also found that increasing the concentration of high-Z elements in metallic glasses resulted in lower MSP values. Mhareb et al. [24] reported that increasing the BaO content in multicomponent borate glasses led to decreases in MSP, SR, and particle range values.

The interactions of polyvinyl chloride (PVC), a widely used polymer, with photon radiation such as gamma rays and X-rays have been extensively investigated, and numerous studies have been reported in the literature. However, studies examining the effects of charged particles, including alpha particles, electrons, and protons, on PVC remain limited. This highlights a significant research gap in understanding the behavior of PVC under different radiation environments. Therefore, in contrast to previous studies, the radiation interaction properties of PVC for electrons, protons, and He^{+2} were investigated over the energy range of 0.001–10,000 MeV. The NIST-based ESTAR, PSTAR, and ASTAR codes were used to calculate the total stopping power (TSP), range, detour factor, density effect parameter, and radiation yield. In addition, the Surrey University Sputter Profile Resolution from Energy Deposition (SUSPRE) code was employed to evaluate the energy deposited by 100 MeV He^{+2} ions in PVC and to determine the depth-dependent ion concentration profiles.

The novelty of this study lies in the systematic comparison of results obtained from these programs, the comprehensive analysis of stopping power and range behavior across different particle types and energy regimes, and the correlation of these findings with the intrinsic material properties.

2. Materials and Analysis

2.1. Materials

The chemical representation of the solid white polymer material produced by the polymerization of polyvinyl chloride monomers is shown in Figure 1.

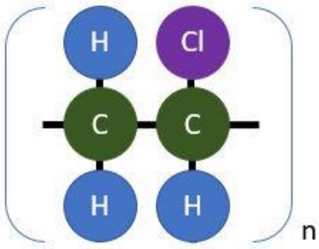

Figure 1. Chemical structure of polyvinyl chloride ($(–CH_2–CHCl–)_n$).
Şekil 1. Polivinil klorürün ($(–CH_2–CHCl–)_n$) kimyasal kompozisyonu.

2.2. Analysis

The ASTAR, PSTAR, and ESTAR programs are NIST-based computational tools used to calculate stopping power (MeV·cm²/g), range (g/cm²), detour factor, density effect parameter, and radiation yield for elements and composite materials irradiated with He^{+2} ions, protons, and electrons [25–28]. A He^{+2} ion fluence of 1.0×10^{15} ions/cm² at an energy of 100 MeV was simulated using the SUSPRE code [29]. The density and mean excitation energy of PVC are 1.3 g/cm³ and 108.2 electro volt (eV), respectively. Table 1 presents the elemental composition, atomic numbers, and weight percentages of PVC, as obtained from the NIST database.

Table 1. Polyvinyl chloride.
Tablo 1. Polivinil klorür.

Composition		
Atom name	**Atomic number**	**Fraction by weight**
H	1	0.048
C	6	0.384
Cl	17	0.567

Stopping power is one of the most important parameters for materials developed to protect against heavy radioactive particles such as protons, electrons, and He^{+2} particles. Total stopping power (TSP) and range are key parameters necessary to understand the collision-stopping interaction mechanism and its attenuation within a given material. Equation 1 provides the TSP formulas for electrons, while Equation 2 provides the TSP formulas for protons and He^{+2} particles.

TSP=Scollision+Sradiative (1)

TSP=Scollision+Snuclear (2)

In a shielding material, the R range of a charged particle, that is, the CSDA value that determines the thickness of a shielding material that a charged particle can penetrate, is given in Equation 3 [30]. The Detour Factor parameter for a shielding material is calculated as in Equation 4 [26].

$$R_{CSDA} = \int_0^E \frac{dE}{S_{tot}} \quad (3)$$

Detour Factor=projected range /CSDA (4)

3. Results and Discussion

Total Stopping Power

The stopping power of the polyvinyl material against proton, electron and He^{+2} are given in Figure 2. The capacities providing the stopping of He^{+2}, electron and protons took the values between $2.369x10^2$ MeV cm^2/g – $1.136x10^2$ MeV cm^2/g; $1.93x10^2$ MeV cm^2/g – $4.04x10^2$ MeV cm^2/g; $1.659x10^2$ MeV cm^2/g – $1.926x10^2$ MeV cm^2/g, respectively. The TSP value for He^{+2} in PVC began to decrease after kinetic energy of 0.7 MeV due to the inability to engage in sufficient Coulomb collisions with alpha scattering. A continuous decrease in TSP values occurred from $3x10^{-2}$ MeV, the initial energy at which the PVC material interacts with the electron, to 1.5 MeV. However, after 1.5 MeV, the TSP values increased again.

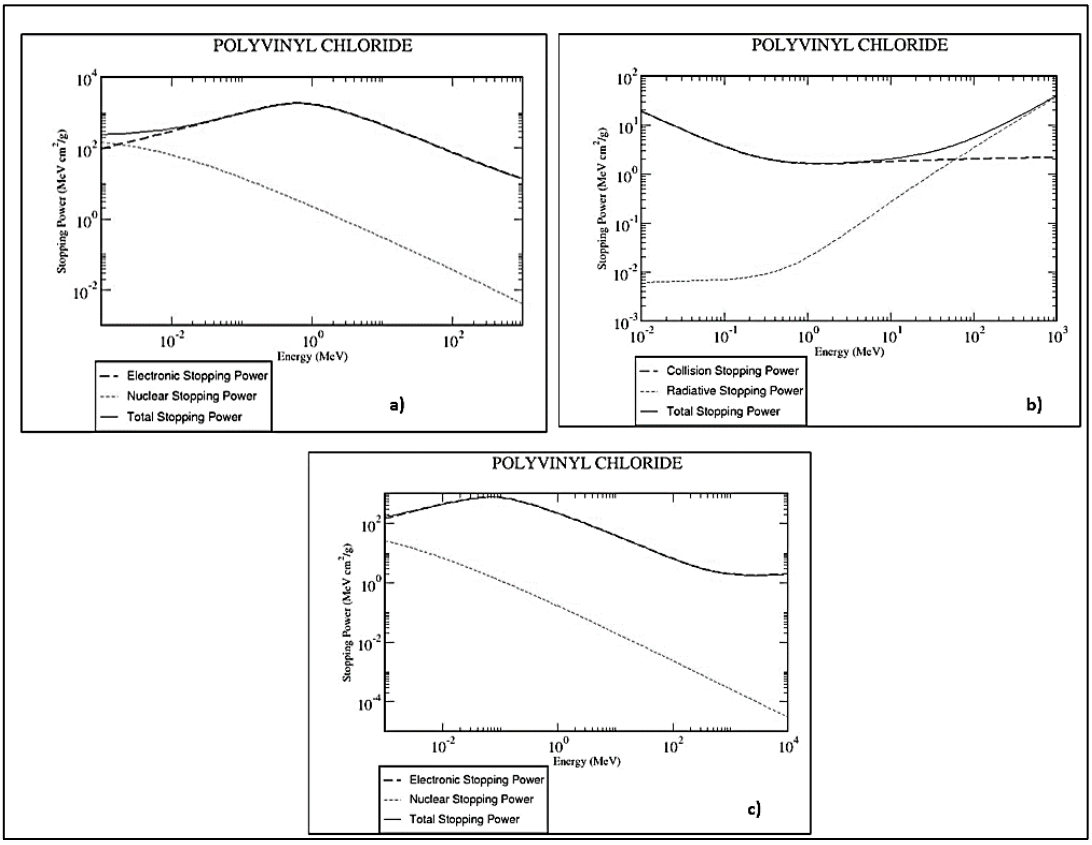

Figure 2. TSP graphs of polyvinyl chloride: a) ASTAR b) ESTAR c) PSTAR.

Şekil 2. Polivinil klorürün TSP grafikleri: a) ASTAR, b) ESTAR, c) PSTAR.

This indicates that the TSP value of the PVC material at high electron energies is higher than the total stopping power at low electron energies. In proton radiation, the TPS started to decrease after a proton energy of $7.5x10^{-2}$ MeV. At 0.02 MeV energy, the TSP values of the PVC material against He^{+2}, electron, and proton particles are $3.549x10^2$ MeV cm^2/g - $1.93x10^1$ MeV cm^2/g, and $4.352x10^2$ MeV cm^2/g, respectively. At 1 MeV energy, they obtained TSP values of $1.710x10^3$ MeV cm^2/g - 1.653 MeV cm^2/g and $2.151x10^2$ MeV cm^2/g. Since He^{+2} and proton particles are heavily charged particles, they exhibit similar behaviour within the PVC material. Due to the fact that electrons are lightly charged particles and their interactions in the electric field, the TSP behaviour is higher at high kinetic energies compared to electrons with low kinetic energies. These data show us that polyvinyl chloride material has the best stopping ability against alpha particles, while its worst stopping ability is against electron particles.

Range

Figure 3 presents the range values (g/cm^2) of protons, electrons, and He^{+2} in PVC. Although protons and electrons may possess the same kinetic energy, their interaction behaviour in PVC differs significantly because of their different masses, charges, and energy-loss mechanisms. In particular, a proton is approximately 1836 times more massive than an electron, resulting in substantially different penetration characteristics. Consequently, different range values are expected for these particles in PVC, as clearly illustrated in Figure 3. For He^{+2} and protons, both the CSDA range and projected range are reported, whereas only the CSDA range is presented for electrons. The CSDA range represents the average path length travelled by a charged particle as it continuously loses energy within a material. The projected range corresponds to the average penetration depth of the particle along its initial direction of motion. The range values of He^{+2}, electrons, and protons increase with increasing kinetic energy because higher-energy particles experience lower stopping power and can therefore penetrate deeper into the material. For electrons, the CSDA range in PVC varies from 2.974 × 10^{-4} g/cm² to 8.247 × 10^{1} g/cm² over the investigated energy range.

The CSDA range values of proton particles vary between 7.734x10^{-6} g/cm^2 and 5.246x10^{3} g/cm^2, while the projected range values vary between 3.127x10^{-6} g/cm^2 and 5.244x10^{3} g/cm^2. The CSDA range values of He^{+2} vary between 4.848x10^{-6} g/cm^2 and 4.331x10^{1} g/cm^2, while the projected range values vary between 2.065x10^{-6} g/cm^2 and 4.329x10^{1} g/cm^2. A high range value of a material selected as a shielding material indicates that its stopping power against incoming charged particles is low. Table 2 shows some CSDA and projected values of He^{+2} and proton particles in the energy range of 1 MeV to 10 MeV. At all energies between 1 MeV and 10 MeV, the CSDA value of the proton particle is higher than the CSDA and projected values of the alpha particle.

Table 2. Some CSDA and Projected values of He^{+2} and protons in the kinetic energy range of 1 MeV- 10 MeV.
Tablo 2. 1 MeV - 10 MeV kinetik enerji aralığında He^{+2} ve protonların bazı CSDA değerleri.

Kinetic Energy	PSTAR		ASTAR	
MeV	CSDA (g/cm^2)	Projected (g/cm^2)	CSDA (g/cm^2)	Projected (g/cm^2)
1	2.933E-03	2.898E-03	7.232E-04	6.840E-04
2	9.061E-03	9.000E-03	1.398E-03	1.357E-03
3	1.791E-02	1.781E-02	2.264E-03	2.222E-03
4	2.926E-02	2.912E-02	3.325E-03	3.281E-03
5	4.298E-02	4.280E-02	4.581E-03	4.535E-03
6	5.898E-02	5.875E-02	6.024E-03	5.976E-03
7	7.719E-02	7.689E-02	7.647E-03	7.598E-03
8	9.754E-02	9.718E-02	9.446E-03	9.394E-03
9	1.200E-01	1.196E-01	1.141E-02	1.136E-02
10	1.445E-01	1.440E-01	1.355E-02	1.349E-02

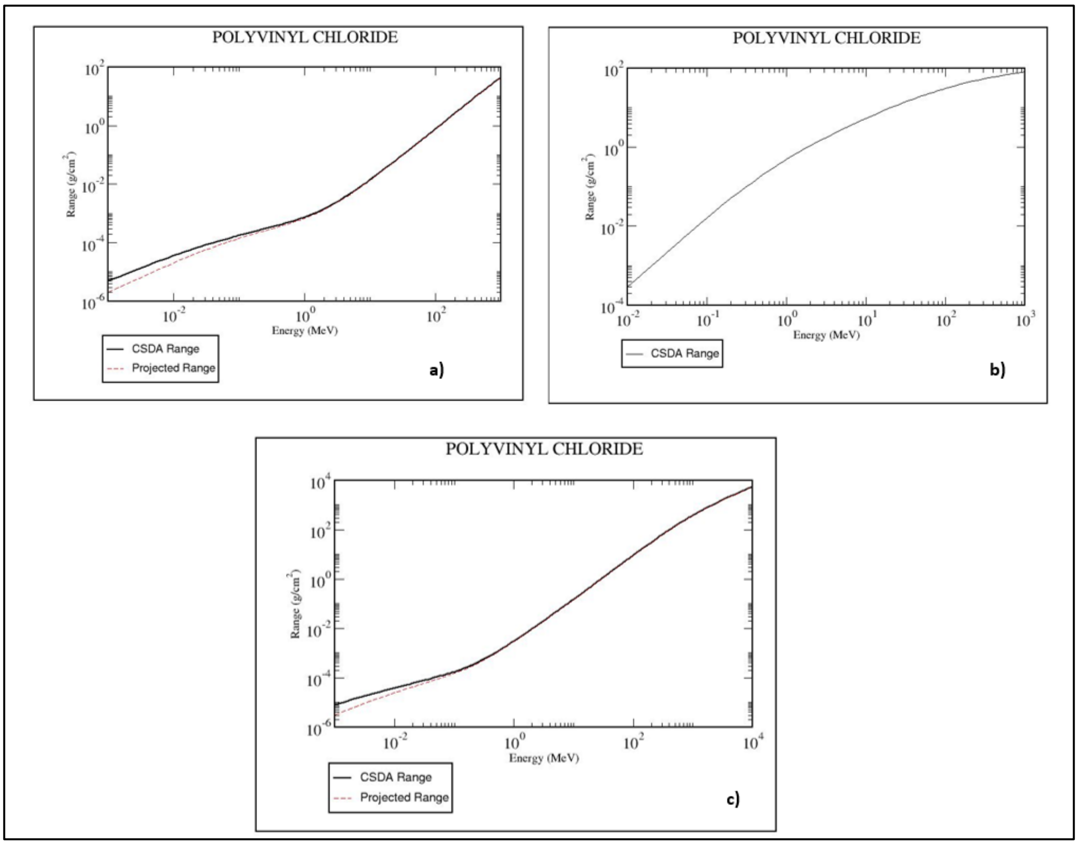

Figure 3: Range graphs of polyvinyl chloride: a) ASTAR b) ESTAR c) PSTAR.
Şekil 3. Polivinil klorürün menzil grafikleri: a) ASTAR b) ESTAR c) PSTAR.

Detour Factor

Figure 4 presents the detour factor values for He^{+2} and protons in PVC. As shown in the figure, the detour factor takes values lower than one across the entire energy range. This behavior arises because He^{+2} and protons do not travel along perfectly straight trajectories within the material due to multiple scattering processes. The detour factor is defined as the ratio of the projected range to the CSDA range. For He^{+2}, the detour factor of PVC is 0.4259 at a kinetic energy of 1×10^{-3} MeV. The detour factor begins to approach a constant value at approximately 25 MeV and becomes nearly constant above 9×10^{2} MeV, reaching a value of 0.9995. For protons, the detour factor is 0.4044 at a kinetic energy of 1×10^{-3} MeV. The detour factor starts to stabilize at approximately 5 MeV and becomes nearly constant at 1×10^{4} MeV, where it reaches a value of 0.9996. For both He^{+2} and protons, the detour factor increases with increasing kinetic energy. This trend indicates that the difference between the actual path length traveled by the particles and their penetration depth decreases as particle energy increases. At high energies, the particle trajectories become increasingly forward-directed, resulting in projected ranges that approach the corresponding CSDA ranges.

Table 3 shows some detour factor values for He^{+2} and protons in the energy range of 1 MeV to 1000 MeV. Because the ASTAR program analyzes the energy range of $1x10^{-3}$ MeV and $1x10^{3}$ MeV, it does not have a detour factor value for the He^{+2} particle at $5x10^{3}$ and $1x10^{4}$ MeV. From 50 MeV onward, the detour factor values for the He^{+2} particle are greater than those for the proton particle. This indicates that the He^{+2} begins to scatter in a flatter orbit from 50 MeV onward.

Table 3: Some Detour Factor values of He^{+2} and protons in the kinetic energy range of 1 MeV- 10^{4} MeV.
Tablo 3. 1 MeV-10^{4} MeV kinetik enerji aralığında He^{+2} ve protonların bazı Sapma Faktör değerleri.

Kinetic Energy	Detour Factor	
MeV	ASTAR	PSTAR
1	0.9459	0.9881
10	0.9959	0.9965
50	0.9989	0.9974
100	0.9992	0.9976
500	0.9994	0.9983
$1x10^{3}$	0.9995	0.9986
$5x10^{3}$	-	0.9999
10^{4}	-	1.0000

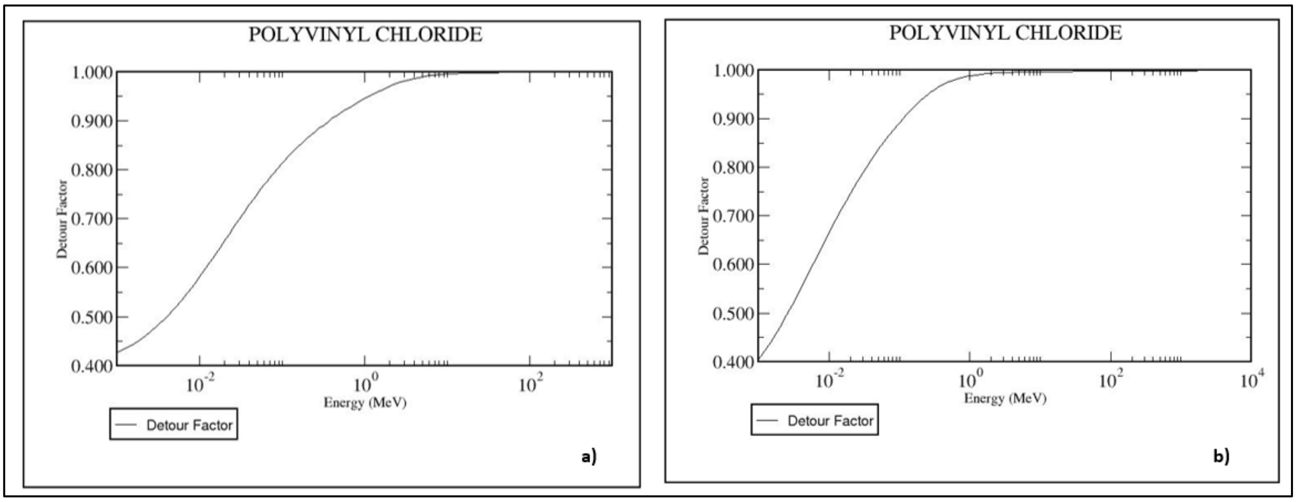

Figure 4. Detour factor graphs of polyvinyl chloride: a) ASTAR b) PSTAR.
Şekil 4. Polivinil klorürün sapma faktör grafikleri: a) ASTAR b) PSTAR.

Density Effect Parameter and Radiation Yield

Figure 5 shows the density effect parameter and radiation yield graphs for PVC material against electron particles. The density effect parameter represents the decrease in collision stopping power of the polyvinyl chloride material due to incident electron particles. Radiation yield represents the average fraction of the initial kinetic energy of an electron that is converted into bremsstrahlung energy as the electron particle decelerates, losing its kinetic energy. In the energy range of $1x10^{-2}$ MeV to $1x10^{3}$ MeV, the density effect parameter and radiation yield values for PVC material range from $1.617x10^{-4}$ to $8.324x10^{-1}$ and 0 to $1.111x10^{1}$, respectively. The radiation yield value of the PVC material increased with the increase in the kinetic energy of the electron.

Energy Deposited and Concentration

Figure 6 shows the depth-dependent concentration graph and the depth-dependent nuclear and electronic energy losses of the PVC material analyzed in the SUSPRE program. The He ion concentration value is zero up to a depth of approximately 8231574 Å. After this value, the He ion implantation rate increases linearly up to a depth of approximately 6.00E+07 Å, while the concentration values increase parabolically after this energy level. An examination of the depth-dependent concentration graph reveals a maximum concentration value at a depth of approximately 71807350 Å. After this depth, the amount of He ion implantation decreases with increasing depth. At a depth of approximately 87394800 Å, the helium ion exhausts its kinetic energy and completes the interaction mechanism within the PVC material. An examination of the depth-dependent energy deposit graph, that is, the depth-dependent nuclear and electronic energy losses of the PVC material, reveals that the changes in the amount of energy lost as a result of electronic interactions with increasing depth vary at very small increments. Energy losses due to nuclear interactions are more linear up to a depth of approximately 5.00E+7E Å, while after this depth the energy losses increase parabolically.

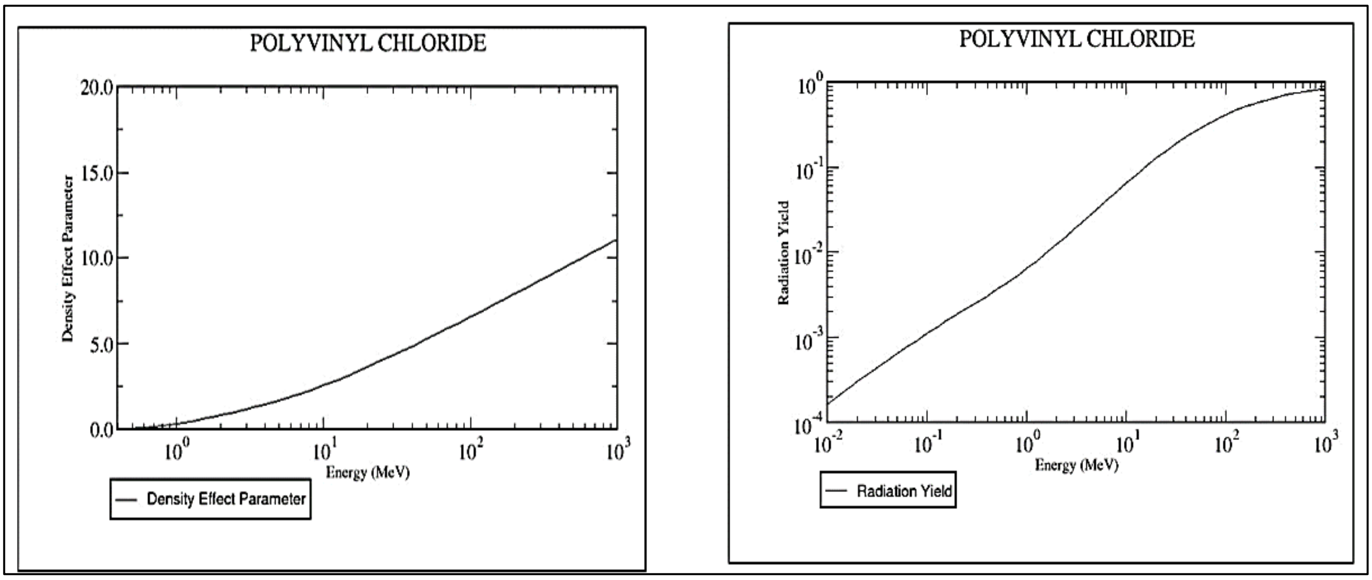

Figure 5. Density effect parameter and radiation yield graphs of polyvinyl chloride.
Şekil 5. Polivinil klorürün yoğunluk etki parametresi ve radyasyon verim grafikleri.

Table 4 shows the energy lost by the PVC material at various depths due to nuclear and electronic interactions. At depths between 86343960.8 Å and 87394800.1 Å, the nuclear and electronic energy losses of the helium ion are zero. This shows that at these depths, the interaction between the helium ion and the PVC material stops at 86343960.8 Å but continues to the depth of 87394800.1 Å due to the helium ion's energy. Because the helium ion is an alpha, it loses its energy through electronic interactions rather than nuclear interactions. However, the high energy of the helium ion introduced caused a loss of energy due to nuclear interactions.

Numerous studies have been reported in the literature on enhancing the radiation attenuation and shielding performance of polymer-based materials. These investigations primarily focus on incorporating high atomic number fillers into polymer matrices to improve the attenuation of ionizing radiation, particularly X-rays and gamma rays. Radiation shielding performance has been evaluated using parameters such as the mass attenuation coefficient (MAC), half-value layer (HVL), etc. The findings indicate that the type, concentration, and dispersion of the filler within the polymer matrix significantly influence the radiation attenuation capability of the resulting composites. Table 5 summarizes selected studies on polymer-based radiation shielding materials reported in the literature.

4. Conclusion

Polyvinyl chloride (PVC) was first analyzed using the NIST database using the ESTAR/ASTAR/PSTAR programs and the SUSPRE simulation program to investigate the behavior of PVC against various ionizing radiations. The ESTAR/ASTAR/PSTAR programs investigated the behavior of particles (protons, alpha particles, and electrons) in the energy range of 0.001 MeV to 104 MeV. The study examined total stopping power (TSP), range, detour factor, density effect parameter, and radiation yield parameters, as well as the change in energy deposited by a 100 MeV He ion with depth and concentration values that change with depth.

• The study shows that the total stopping power of polyvinyl chloride against electrons, alpha particles, and protons decreases with increasing energy.
• Among the investigated particle types, polyvinyl chloride exhibited the highest shielding performance against alpha particles, whereas its lowest shielding performance was observed against electrons.

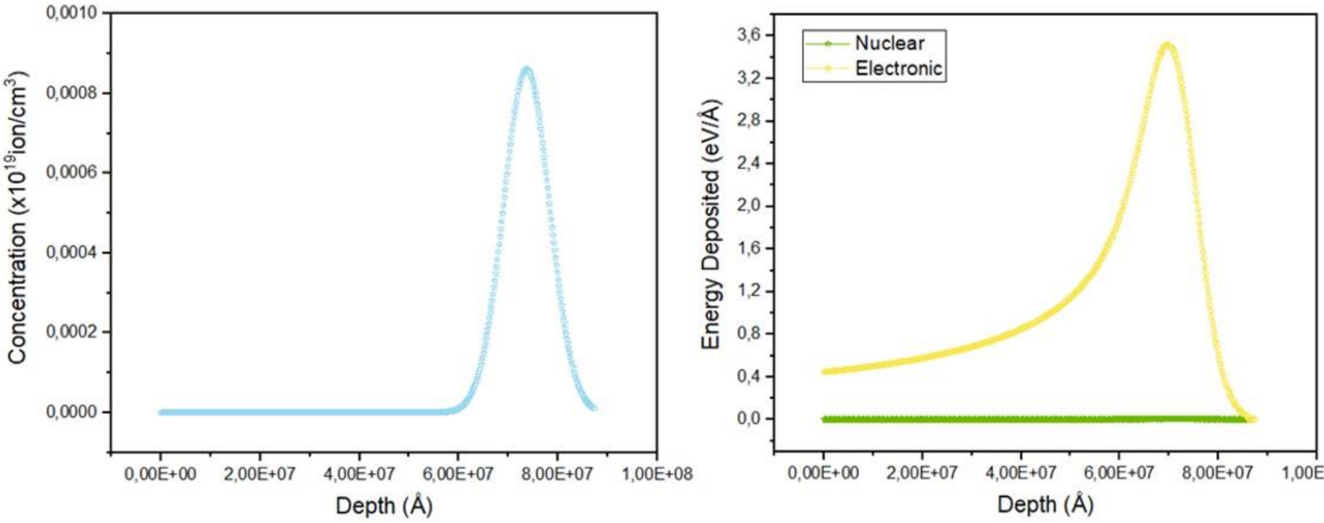

Figure 6. PVC data from the SUSPRE program.
Şekil 6. SUSPRE programından elde edilen PVC verileri.

Table 4. Energy losses depending on depth.
Tablo 4. Derinliğe bağlı enerji kayıpları.

Depth (Å)	Nuclear (eV/ Å)	Electronic (eV/ Å)	Depth (Å)	Nuclear (eV/ Å)	Electronic (eV/ Å)
0	0.000222	0.445228	24694723.1	0.000321	0.62184
175139.88	0.000223	0.44598	24869863	0.000322	0.623705
350279.76	0.000223	0.446734	25395282.6	0.000326	0.629375
525419.64	0.000223	0.447491	25570422.5	0.000327	0.63129
700559.52	0.000224	0.448251	25745562.4	0.000328	0.633218
875699.4	0.000224	0.449014	29248360	0.000352	0.674698
1050839.28	0.000225	0.44978	43609830.1	0.000509	0.93614
2451958.32	0.000228	0.456008	43784970	0.000512	0.940768
2627098.2	0.000228	0.456801	43960109.9	0.000515	0.945448
2802238.08	0.000229	0.457597	54293362.8	0.000789	1.367738
2977377.96	0.000229	0.458399	54468502.7	0.000797	1.378951
3152517.84	0.00023	0.459207	54643642.6	0.000805	1.39039
3327657.72	0.00023	0.460022	54818782.4	0.000813	1.402064
3502797.6	0.000231	0.460848	54993922.3	0.000821	1.41398
3677937.48	0.000231	0.461685	68829972.8	0.003425	3.48302
3853077.36	0.000232	0.462538	69005112.7	0.003474	3.495145
4028217.24	0.000232	0.463407	69180252.6	0.003521	3.50485
19265386.8	0.000291	0.569508	69355392.5	0.003567	3.512045
19440526.7	0.000292	0.571046	69530532.4	0.00361	3.516648
19615666.6	0.000293	0.572593	69705672.2	0.003651	3.518582
19790806.4	0.000294	0.574149	69880812.1	0.003689	3.517779
19965946.3	0.000295	0.575715	79513505.5	0.00135	0.723107
20141086.2	0.000296	0.57729	79688645.4	0.001284	0.680103
20316226.1	0.000297	0.578874	79863785.3	0.001221	0.638888
20491366	0.000298	0.580468	80038925.2	0.001159	0.599453
20666505.8	0.000299	0.582072	80214065	0.001099	0.561783
20841645.7	0.0003	0.583685	84767701.9	0.000248	0.071324
21016785.6	0.0003	0.585308	85293121.6	0.000236	0.052614
21191925.5	0.000301	0.586941	85468261.4	0.00024	0.046666
21367065.4	0.000302	0.588584	85643401.3	0.000252	0.04051
21542205.2	0.000303	0.590238	85818541.2	0.000279	0.033787
21717345.1	0.000304	0.591901	85993681.1	0.000341	0.025967
21892485	0.000305	0.593575	86168821	0.000552	0.015807
24169303.4	0.000318	0.616317	86343960.8	0	0
24344443.3	0.000319	0.618146	87044520.4	0	0
24519583.2	0.00032	0.619987	87394800.1	0	0

Table 5: Literature review.
Tablo 5: Literatür taraması.

Materials	Type of radiation	Energy	Parameters	Value	Ref.
PW5% -P35% (%60PVC +%35PbO + 5%WO3	Gamma	^{241}Am	MAC	1.6646 ±0.078 cm^2/g	[19]
PVC-50HfC (in GEANT4 program)	Gamma	1 MeV	MAC	0.0656 cm^2/g	[20]
LDPE/PVC/ $MgCo_2O_4$	He^{+2}	10^{-4} MeV	MSP	~ 60 MeVcm^2/g	[21]
LDPE/PVC/ Al_2CoO_4	Proton	10^{-4} MeV	MSP	~17 MeVcm^2/g	[21]
MG6 ($Ca_{65}Mg_{15}Zn_{20}$)	Alpha	1 MeV	MSP	~1.1 MeVcm^2/g	[23]
MG6 ($Ca_{65}Mg_{15}Zn_{20}$)	Proton	1 MeV	MSP	~0.15 MeVcm^2/g	[23]
10%ZnO+10%Na_2O+50%H_3BO_3+30%BaO	Proton	7 MeV	MSP	~0.4 MeVcm^2/g	[24]
10%ZnO+10%Na_2O+50%H_3BO_3+30%BaO	Gamma	0.184	MAC	1.3949 cm^2/g	[24]

5. Conflicts of Interest

There is no conflict of interest.

6. References

[1] Kavun, Y., Eskalen, H., Kavgacı, M., 'A study on gamma radiation shielding performance and characterization of graphitic carbon nitride', Chemical Physics Letters 811 (2023) 140246, https://doi.org/10.1016/j.cplett.2022.140246

[2] Tyagi, G., Singhal, A., Routroy, S., Bhunia, D., Lahoti, M., 'Radiation Shielding Concrete with alternate constituents: An approach to address multiple hazards', Journal of Hazardous Materials 404 (2021) 124201, https://doi.org/10.1016/j.jhazmat.2020.124201

[3] Lardhi, M., Mukhtar, F., 'Radiation shielding performance of seawater-mixed concrete incorporating recycled coarse aggregate and steel slag', Journal of Radiation Research and Applied Sciences 16 (2023) 100528, https://doi.org/10.1016/j.jrras.2023.100528

[4] Gashti, M.F., Mousavinejad, S.H.G., 'Evaluation of gamma and neutron radiation shielding properties of the GGBFS based geopolymer concrete', Construction and Building Materials 367 (2023) 130308, https://doi.org/10.1016/j.conbuildmat.2023.130308

[5] Beyazay, E., Karabul, Y., Korkut, S.E., Kılıç, M., Özdemir, Z.G., 'Multifunctional PCz/BaO nanocomposites: Ionizing radiation shielding ability and enhanced electric conductivity, Progress in Nuclear Energy 155 (2023) 104521, https://doi.org/10.1016/j.pnucene.2022.104521

[6] Kavun, Y., Kamer, M.S. (2026). Effect of line width and layer height variation on radiation shielding properties of 3D-printed poly(lactic acid) materials. Radiation Physics and Chemistry 240 (2026) 113410. https://doi.org/10.1016/j.radphyschem.2025.113410

[7] Mahmoud, K.A., Lacomme, E., Sayyed, M.I., Özpolat, Ö.F., Tashlykov, O.L. (2020). Investigation of the gamma ray shielding properties for polyvinyl chloride reinforced with chalcocite and hematite minerals. Heliyon 6 (2020) e03560. https://doi.org/10.1016/j.heliyon.2020.e03560

[8] You, J., Cai, Yu, R., Xing, H., Xue, J., Li, Y., Jiang, Z., Cui, D., Tang, T. (2024). High-performance chlorinated polyvinyl chloride/polyurea nanocomposite foam with excellent solvent resistance, flame-triggered shape memory effect and its upcycling. Composites: Part A 177 (2024) 107931. https://doi.org/10.1016/j.compositesa.2023.107931

[9] Zheng, D., Li, J., Yu, B., Yang, Y., Huang, Z., Zhang, Y., Liu, C. (2024). Grand canonical Monte Carlo and molecular dynamics investigation of hydrogen solubility and diffusivity in nonmetallic polyvinyl chloride, polyethylene and polyvinylidene fluoride pipes materials. Fuel 362 (2024) 130925. https://doi.org/10.1016/j.fuel.2024.130925

[10] Huang, Z., Sun, M., Zheng, Y., Han, Y., Liu, H., Shen, J., (2023). A micro sample pretreatment technique combined with ion chromatography and its application in the determination of polyvinyl chloride. Journal of Chromatography A 1690 (2023) 463778. https://doi.org/10.1016/j.chroma.2023.463778

[11] El-Seidy, E., Sambucci, M., Chougan, M., Al-Noaimat, Y.A., Al-Kheetan, M.J., Biblioteca, I., Valente, M., Ghaffar, S.H. (2023). Alkali activated materials with recycled unplasticised polyvinyl chloride aggregates for sand replacement. Construction and Building Materials 409 (2023) 134188. https://doi.org/10.1016/j.conbuildmat.2023.134188

[12] El-Mesady, I., El-Agawany, F.I., El-Samman, H., Hussein, A., Rammah, Y.S., Elsad, R.A. (2023). Synthesis, optical characteristics, and gamma-ray protection competence evaluation of polyvinyl chloride reinforced basalt nanocomposites. Radiation Physics and Chemistry 212 (2023) 111122. https://doi.org/10.1016/j.radphyschem.2023.111122

[13] Issa, S.A.M., Abulyazied, D.E., Alrowaily, A.W., Saudi, H.A, Ali, E.S., Henaish, A.M.A., Zakaly, H.M.H. (2023). Improving electrical, optical and radiation shielding properties of polyvinyl alcohol yttrium oxide composites. Journal of Rare Earths 41 (2023) 2002-2009. https://doi.org/10.1016/j.jre.2023.02.013

[14] Chang, Q., Guo, S., Zhang, X. (2023). Radiation shielding polymer composites: Ray interaction mechanism, structural design, manufacture and biomedical applications. Materials & Design 233 (2023) 112253. https://doi.org/10.1016/j.matdes.2023.112253

[15] Issa, S.A.M., Alrowaily, A.W., Oche, C., Henaish, A.M.A., Halaka, M.M.A., Alatawi, N.S., Zakaly, H.M.H. (2023). Unveiling the potentials of polyvinyl alcohol/manganese chloride nanocomposites films: A detailed examination of their structural, spectral, and radiation properties. Materials Today Communications 37 (2023) 107177 https://doi.org/10.1016/j.mtcomm.2023.107177

[16] Ihsani, R.N., Gareso, P.L., Tahir, D. (2024). An overview of gamma radiation shielding: Enhancements through polymer-lead (Pb) composite materials. Radiation Physics and Chemistry 218 (2024) 111619. https://doi.org/10.1016/j.radphyschem.2024.111619

[17] Aldawood, S., Asemi, N.N., Kassim, H., Aziz, A.A., Saeed, W.S., Al-Odayni, A.B. (2024). Gamma radiation shielding by titanium alloy reinforced by polymeric composite materials. Journal of Radiation Research and Applied Sciences 17 (2024) 100793. https://doi.org/10.1016/j.jrras.2023.100793

[18] Yılmaz, M., Akman, F. (2023). Gamma radiation shielding properties for polymer composites reinforced with bismuth tungstate in different proportions. Applied Radiation and Isotopes 200 (2023) 110994. https://doi.org/10.1016/j.apradiso.2023.110994

[19] Darki, S.P., Kalantari, M.E., Zare, H., Arani, A.R.M. (2025). Preparation and structural characterization of PbO and WO3-PVC hybrid nanocomposites for gamma-ray radiation shielding. Radiation Physics and Chemistry 229 (2025) 112489. https://doi.org/10.1016/j.radphyschem.2024.112489

[20] Hadjal, A., Saim, A., Akman, F., Özdoğan, H., Dib, A.S.A., Tebboune, A. (2026). Monte Carlo study of gamma radiation shielding capabilities of PVC-based composites reinforced with heavy transition metal carbides. Nuclear Instruments and Methods in Physics Research B 573 (2026) 166045. https://doi.org/10.1016/j.nimb.2026.166045

[21] Mansy, M.S., Ghobashy, M.M., Aly, M.I. (2024). Enhancing gamma and neutron radiation shielding efficiency of LDPE/PVC polymers using cobalt, aluminum, and magnesium oxide fillers.

Radiation Physics and Chemistry 222 (2024) 111862. https://doi.org/10.1016/j.radphyschem.2024.111862

[22] Tahir, D., Sari, S.N.H., Yulianti (2015). Stopping powers and inelastic mean free path of 200eV–50 keV electrons in polymer PMMA, PE, and PVC. Applied RadiationandIsotopes95(2015)59–62. http://dx.doi.org/10.1016/j.apradiso.2014.10.001

[23] Perişanoğlu, U. (2019). Assessment of nuclear shielding and alpha/proton mass stopping power properties of various metallic glasses. Applied Physics A (2019) 125:801. https://doi.org/10.1007/s00339-019-3105-8

[24] Mhareb, M.H.A., Alajerami, Y.S.M., Dwaikat, N., Al-Buriahi, M.S., Alqahtani, M., Alshahri, F., Saleh, N., Alonizan, N., Saleh, M.A., Sayyed, M.I. (2021). Investigation of photon, neutron and proton shielding features of H3BO3-ZnO-Na2O-BaO glass system. Nuclear Engineering and Technology 53 (2021) 949-959. https://doi.org/10.1016/j.net.2020.07.035

[25] Berger, M.J., Coursey, J.S., & Zucker, M.A. (1999). ESTAR, PSTAR, and ASTAR: computer programs for calculating stopping-power and range tables for electrons, protons, and helium ions (version 1.21). http://physics.nist.gov/Star

[26] ESTAR, PSTAR, ASTAR, National Institute of Standards and Technology (NIST), and ICRU Report 49, International Commission on Radiation Units and Measurements, Bethesda, MD, USA, 1993 https:// www.nist.gov/

[27] Berger M.J., Coursey J.S., Zucker M.A., Chang J. Stopping-power & range tables for electrons, protons, and helium ions, NIST standard reference database; 2017. https://physics.nist.gov/PhysRefData/Star/Text/ESTAR.html

[28] Sharma, A., Singh, B., Sandhu, B.S. Investigations on tissue equivalence of selected biomaterials through radiological parameters. Chinese Journal of Physics 84 (2023) 103–118. https://doi.org/10.1016/j.cjph.2023.02.010

[29] Webb, R.P., Wilson, I.H., 1986. An extension to the Projected Range Algorithm (PRAL)to give energy deposition profiles. In: Proc. 2nd Int. Conf. Simulation of Semi-conductor Devices and Processes.

[30] Osman, H., Gümüş, H. (2022). Stopping power and CSDA range calculations of electrons and positrons over the 20 eV–1 GeV energy range in some water equivalent polymer gel dosimeters. Applied Radiation and Isotopes 179 (2022) 110024. https://doi.org/10.1016/j.apradiso.2021.110024